Comprehensive assessment of permafrost carbon emissions indicates need for urgent action to keep Paris Agreement temperature goals within reach

SUPPLEMENTARY INFORMATION

Rachael Treharne, Thomas Gasser, Brendan M. Rogers, Merritt R. Turetsky, Christina Schaedel, Erin MacDonald, Susan Natali

Section S1: Emissions budgets

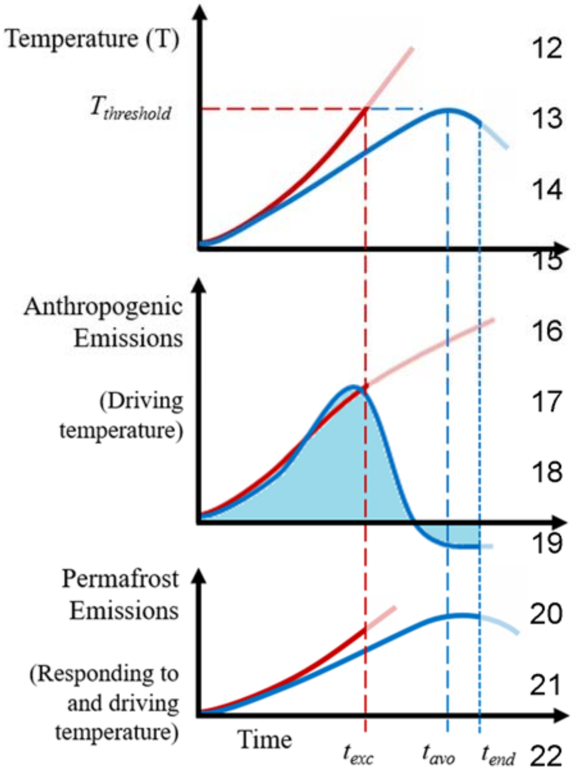

Figure S1.1: Modified from Gasser et al., 2018. Conceptual figure illustrating the exceedance and avoidance budget calculation approaches. Exceedance budgets (red) are the amount of CO_2 that can be emitted before exceeding a given temperature threshold. Avoidance budgets (blue) are the amount of CO_2 that can be emitted while staying below the target. t_{exc} indicates the time at which a specified temperature threshold is exceeded (for exceedance budgets); t_{avo} indicates a temperature peak at the same threshold, in line with a conceptualized avoidance scenario. t_{end} indicates the end of the conceptualized avoidance scenario, beyond which further temperature change is not considered in the corresponding budget calculation. Permafrost emissions are not directly used to calculate emissions budgets, but are included here for comparison. See sections S1.1 and S1.2 for full explanation.

S1.1 Avoidance budgets

Avoidance budgets are the maximum amount of CO_2 that can be emitted while temperatures remain below the specified temperature threshold for the duration of the modeled scenario. To ensure temperatures genuinely remained below the specified threshold, each simulation set (Table 1) was run across a range of pathways under which fossil fuel CO_2 emissions reach a peak and subsequently decline. These ‘peak and decline’ scenarios were obtained by updating the fossil fuel CO_2 emission pathways described in Gasser et al., (2018) to align the historical period and the historical growth rate of CO_2 emissions with the global Shared Socioeconomic Pathways (SSP) data (Meinshausen et al., 2020).

In order to maximize the number of simulations with maximum temperatures within +0.5°C of the specified temperature target, K means clustering was used on an initial set of simulations run across 520 CO_2 emission pathways to select a subset of 176 pathways which were paired with 161 Monte Carlo configurations from a scheme of 500.

S1.2 Exceedance budgets

An exceedance budget is the amount of CO_2 that is emitted before the specified temperature threshold is exceeded ($t_{exc,}$ Fig S1). This type of emissions budget does not consider temperature or temperature drivers (including anthropogenic emissions and earth system feedbacks such as permafrost emissions) subsequent to t_{exc}. Exceedance scenarios are also less aligned with the framing of the Paris Agreement goals, and are therefore used here as a supporting analysis only.

To calculate exceedance budgets, each simulation set (Table 1) was run using a Monte Carlo scheme of 500. The Exceedance budget for each simulation was calculated as the cumulative anthropogenic CO_2 emitted up to the year when additional warming exceeded the specified temperature target.

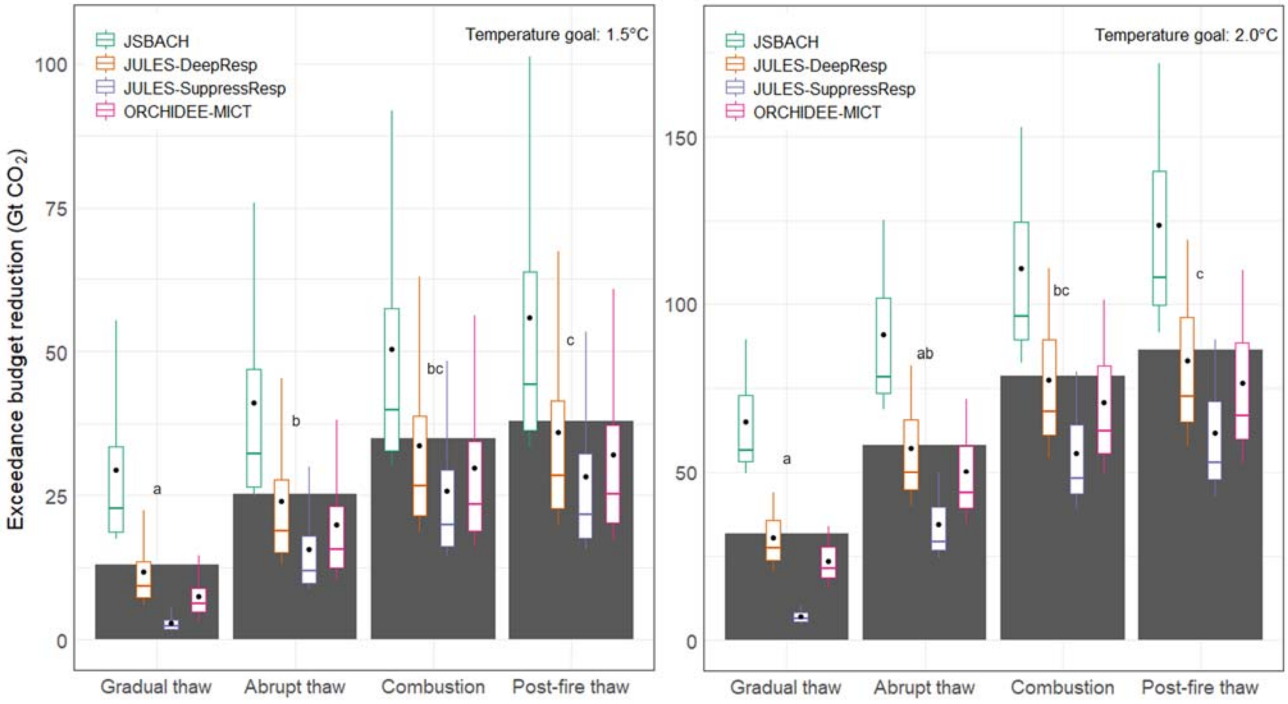

Figure S1.2: Reductions (Gt CO_2) in remaining exceedance budgets for the 1.5°C (left) and 2.0°C (right) temperature goals. The absolute value of the budgets ranged from 449 Gt CO_2 to 675 Gt CO_2 for the 1.5°C threshold, and from 1346 Gt CO_2 to 1716 Gt CO_2 for the 2.0°C threshold (Table S3). Box plots show results for each of the 4 LSMs (black circles indicate the mean value for each LSM), and gray bars represent mean reduction for all 4 LSMs. Annotation of bars with different/matching letters indicates statistically significant differences/lack thereof between those bars ($p<0.05$). Processes are incorporated into model configurations in a stepwise manner, meaning (for example) the abrupt thaw configuration also includes gradual thaw.

S1.3 Observed temperature change during a recent baseline period

We used HadCRUT5 to establish a baseline of 1.138°C of global average temperature increase during the 2012-2021 period (Morice et al., in press). This means we calculated carbon budgets associated with exceeding (section 5.2) or avoiding (section 5.3) an additional 0.362°C (for 1.5°C threshold) or 0.862°C (for 2°C threshold) of global average temperature increase.

Section S2: Temperature response of total burned area

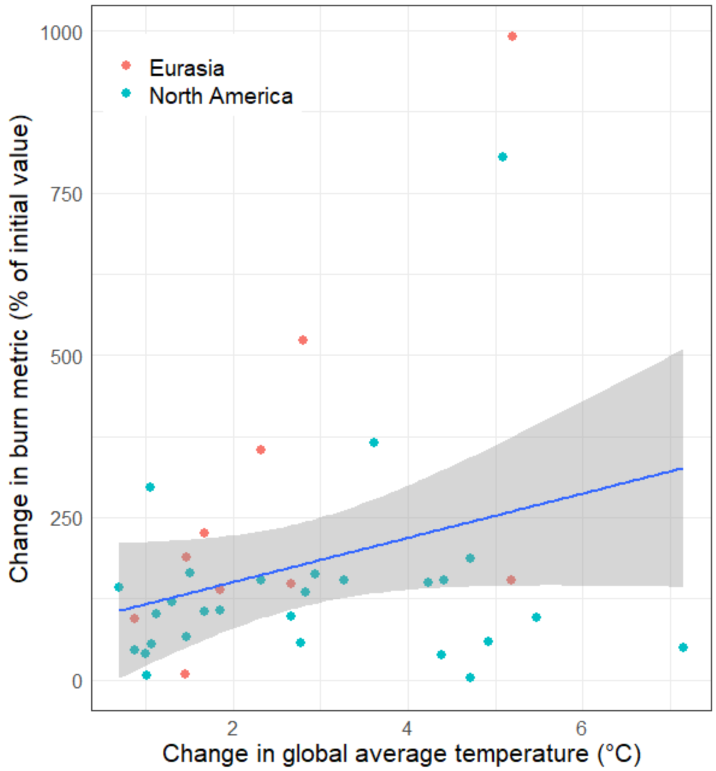

Figure S2.1: Projections of change in burn metric (burned area, carbon emissions or fire frequency) with change in global average temperature for the North American or Eurasian boreal and/or tundra regions, with linear regression (y=34*x + 83; F=3.099, DF=1,36, p=0.087). Each point represents a specific climate scenario. Data obtained through systematic literature review.

S2.1 Systematic literature review for projection of change in burned area

We sought projections of change in burned area, carbon emissions or fire frequency for the North American, Eurasian, or pan-Arctic boreal and/or tundra regions. Our selection process was based on the following criteria: the paper included a projected fire metric (burned area, carbon emissions, or fire frequency were accepted, but weather-based fire metrics such as the Canadian Fire Weather Indices were not) for any year from 2060 to 2100. We excluded any papers that had a sub-regional domain (<~100,000 km2). Our final criterion was that the paper included the corresponding change in global mean temperature or, where temperature change was not explicitly included, enough information about the Global Climate Model and emissions scenario used to retrieve temperature change information for the corresponding time periods. We did not include any papers that manipulated burned area as a factor, nor any that used the same input data as a paper that was already included (as this would result in replicate projections). Our final analysis included 8 papers for North America (Boulanger et al. 2018; Genet et al. 2018; Pastick et al. 2017; Boulanger et al. 2014; Genet et al. 2013; Balshi et al. 2009; Euskirchen et al. 2009;

Bachelet et al. 2005), 2 papers for Eurasia (Kicklighter et al. 2014; Dixon & Krankina, 1993), and 2 papers which included both (pan-Arctic; Eliseev et al. 2014; Kloster et al. 2012).

Because many papers included either multiple regions or multiple Global Climate Models, we weighted estimates so that each paper would have a total weight of one (e.g., if a paper used two Global Climate Models, each estimate was given a weight of 0.5 in the calculation of the final average) to determine our final weighted average of a 0.7517 increase in burn metric °C^{-1} of warming. As this linear temperature response did not differ significantly between North America and Eurasia (p=0.069), a single response was used within the model (fig S2.1).

S2.2 Compensating for increased post-fire NPP

We compensated for increased post-fire NPP by increasing CO_2 uptake relative to emission losses during a set post-fire recovery interval, parameterized based on crown fires in boreal North America.

Fire results in a short-term loss of NPP, followed by a period of increased carbon sequestration as vegetation recovers (Goulden et al., 2011; Randerson et al., 2006). This recovery period begins about 10 years after fire and continues on the timescale of years to decades until the ecosystem reaches a stable successional state, by which point NPP declines to approximately pre-fire levels. This post-fire carbon sink was parameterized to remove a volume of CO_2 equivalent to 100% of that emitted by fire at a rate subject to exponential decay during a conservative fire return interval of 150 years. This 100% ‘offset’ of combustion emissions by enhanced post-fire CO_2 uptake is a typical response of boreal forests following fire (Goulden et al., 2011), and is therefore a realistic assumption in at least some forested permafrost regions. However, in some tundra regions, even NPP of early successional communities is low when compared to the soil carbon stocks vulnerable to combustion (Madani et al., 2021; Loranty et al,. 2014; Mack et al., 2011). Carbon emitted during tundra fire is therefore unlikely to be fully compensated for during recovery, meaning that our estimate of net emissions from tundra fires is likely conservative.

Section S3: Post-fire progressive and temporary thaw

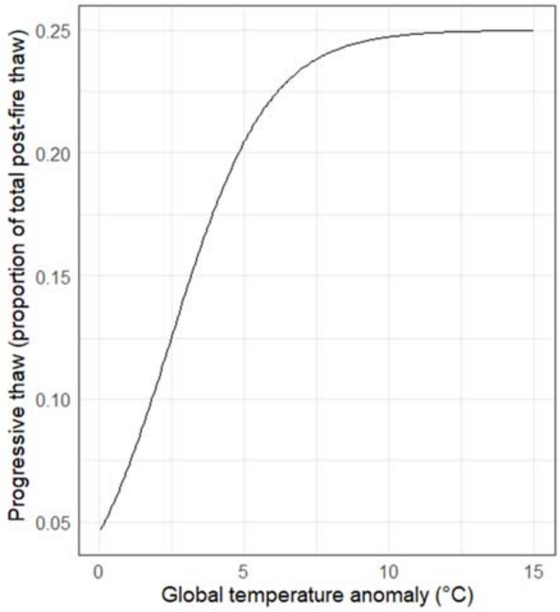

Figure S3.1: Temperature response function applied to remaining burned area (i.e. total burned area, less that affected by post-fire abrupt thaw) to obtain an annual proportion of that area affected by post-fire progressive thaw (methods section 4.2).

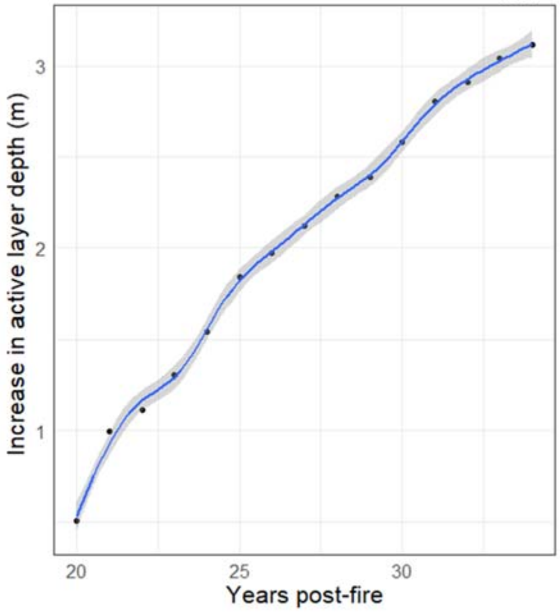

Figure S3.2: Modeled increase in active layer depth following fire in upland boreal forest with dynamic organic soil recovery. Data extracted from Jafarov et al., (2013) and used to estimate the time period for progressive thaw of near-surface (upper 3m) permafrost (methods section 4.2). Estimate made using a General Additive Model (blue line).

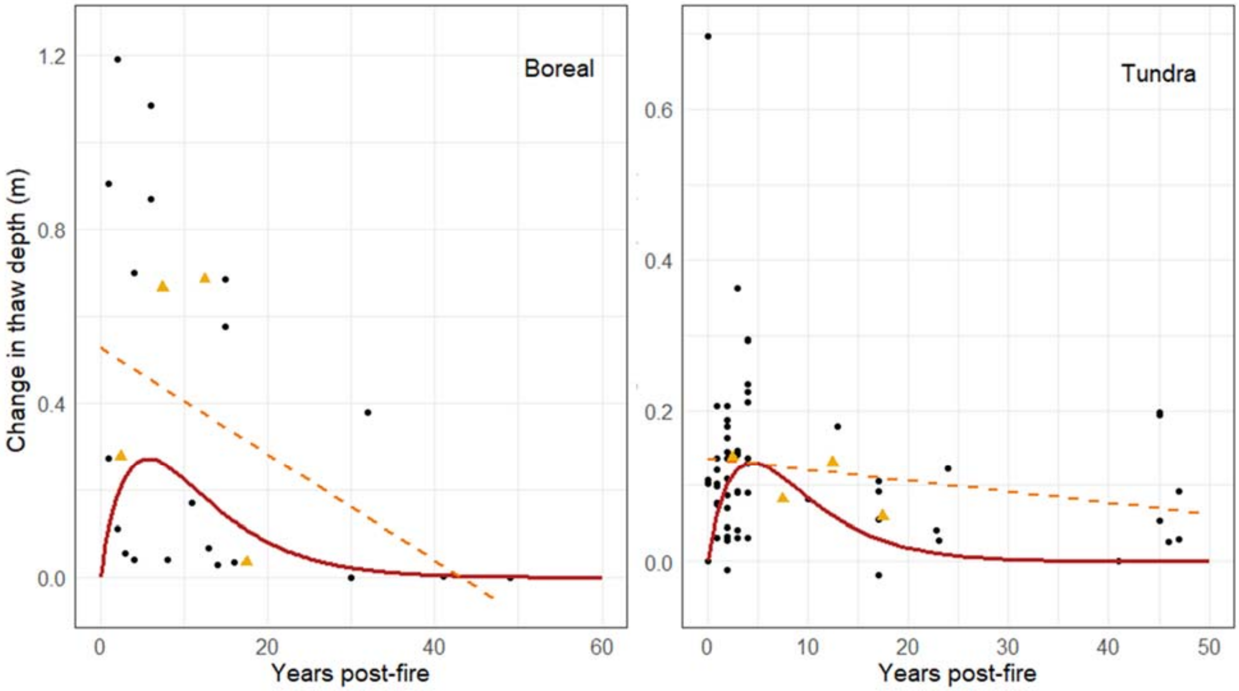

Figure S3.3: Temporary change in active layer depth following fire in tundra (left) and boreal (right) biomes. Points represent observational data obtained by systematic literature review (methods section 4.4). Red lines show the trajectories of change in active layer depth under temporary post-fire thaw. Thaw trajectories were informed by observation data and fitted to meet additional criteria; increase in active layer to peak within 10 years of fire; change in active layer depth must decline to 0 within 50 years of fire; trajectory curve must integrate to a value less than or equal to the corresponding linear regression during the first five years post-fire. For ease of interpretation, golden triangles show 5-year averages and dashed orange lines show linear regression

S3.1 Post-fire progressive and temporary thaw emissions

Emissions associated with both progressive and transient post-fire thaw were calculated following the approach of the gradual thaw permafrost carbon emulator. In brief, the quantities of thawed permafrost carbon, which are output from progressive and transient thaw processes, are split between up to three carbon pools, following the parameterization of the gradual thaw module according to the specified LSM configuration. Each of these pools is subjected to heterotrophic respiration with its own turnover time, and subsequently converted to CO_2 and CH_4 emissions, with the proportion of carbon emitted as CH_4 set at 2.3% (see Gasser et al., 2018 for more detail).

Section S4: Post-fire abrupt thaw

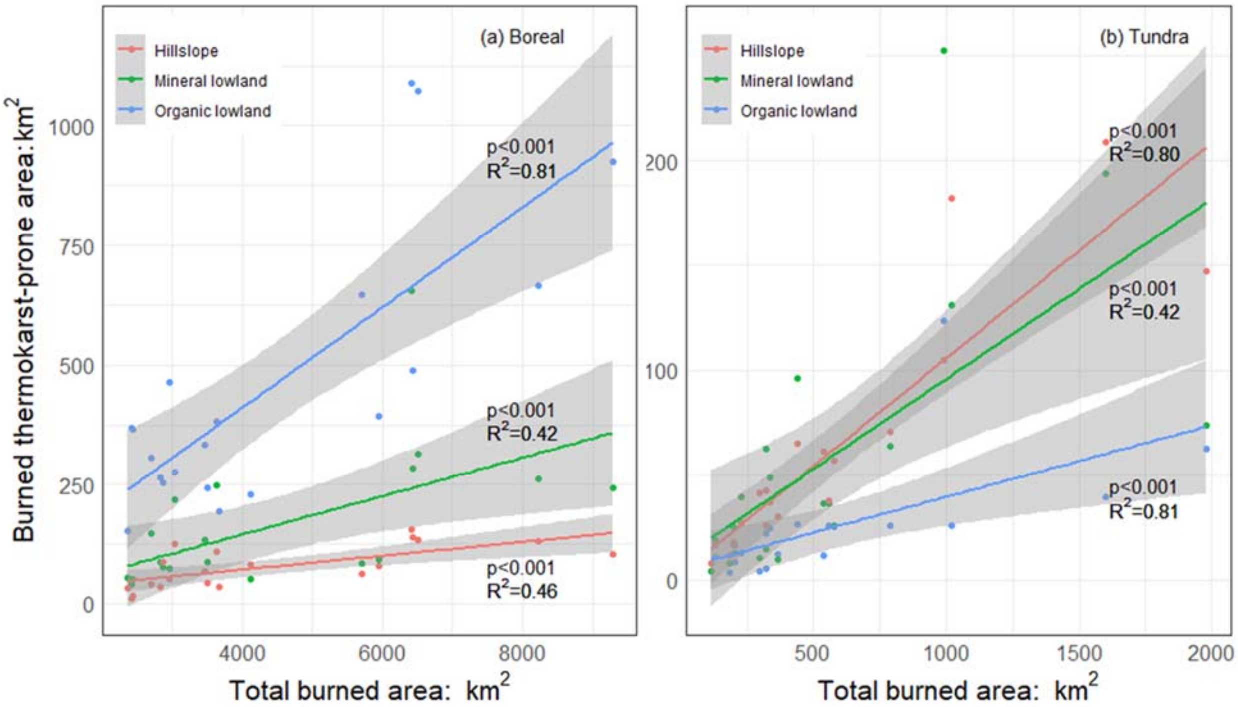

Figure S4.1: Linear correlations between total annual burned area across the (a) boreal and (b) tundra biomes, and annual burned thermokarst-prone area in each biome and in different landscape types from 1997-2016. Data obtained using van der Werf et al., 2017 and Olefeldt et al., 2016.

Section 5: Permafrost and fire related emissions

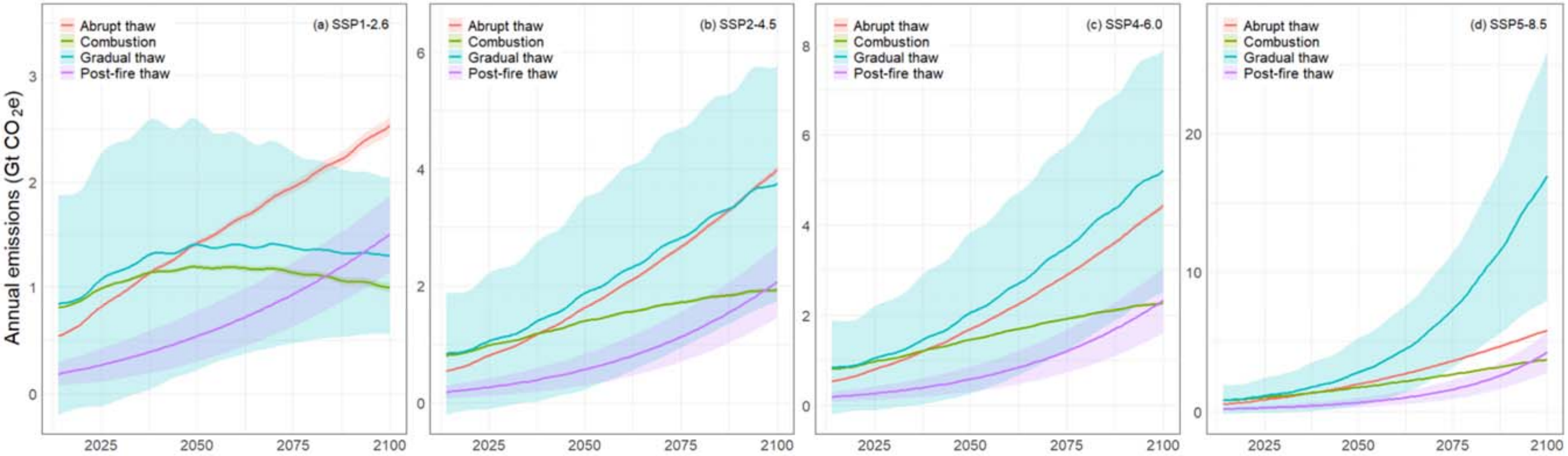

Figure S5.1: Total annual CO2 and CH4 emissions (GtCO2e) under different SSP-RCP scenarios (left to right, high to low mitigation effort) originating from different processes modeled within OSCAR (line colors) from 2014 to 2100. Confidence intervals represent 1 standard deviation.

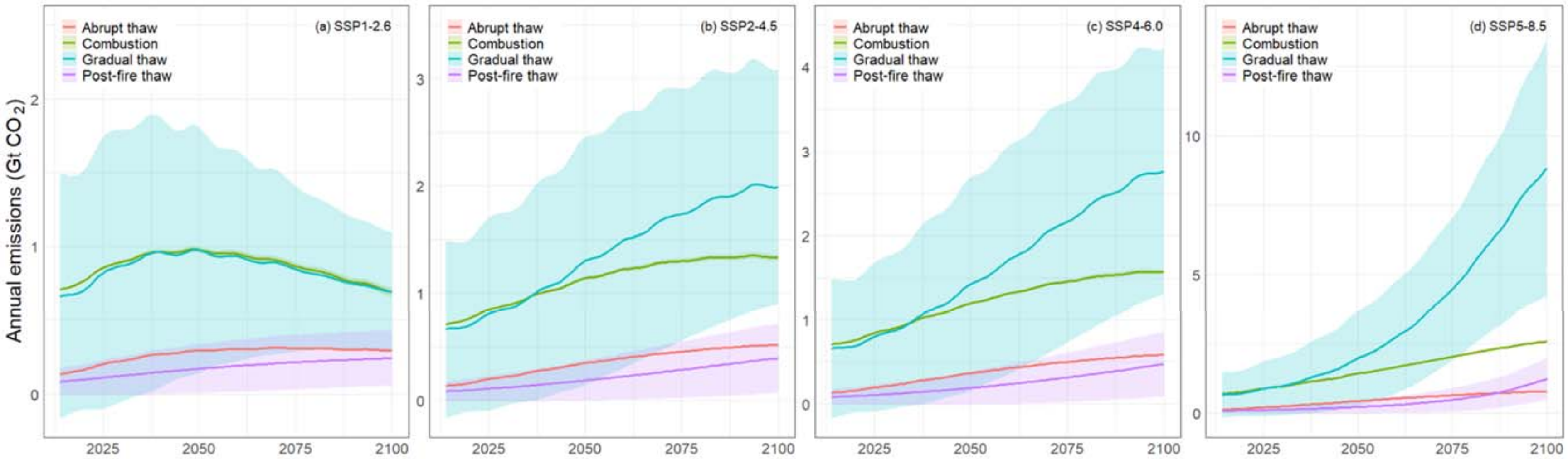

Figure S5.2: Total annual CO2 emissions (GtCO2) under different SSP-RCP scenarios (left to right, high to low mitigation effort) originating from different processes modeled within OSCAR (line colors) from 2014 to 2100. Confidence intervals represent 1 standard deviation.

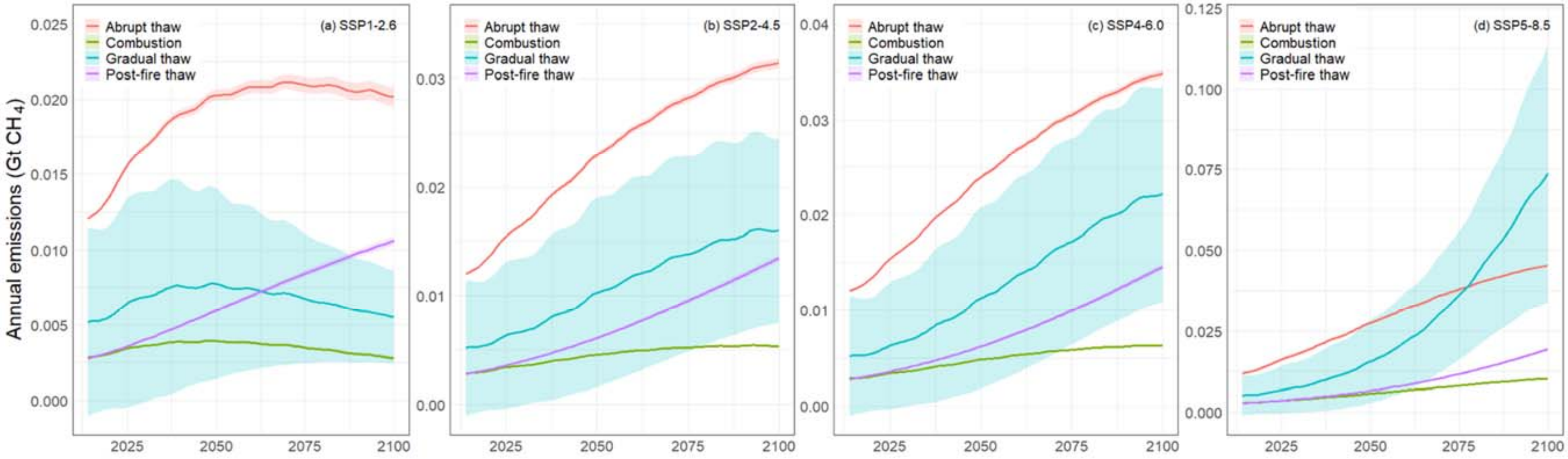

Figure S5.3: Total annual CH4 emissions (GtCH4) under different SSP-RCP scenarios (left to right, high to low mitigation effort) originating from different processes modeled within OSCAR (line colors) from 2014 to 2100. Confidence intervals represent 1 standard deviation.

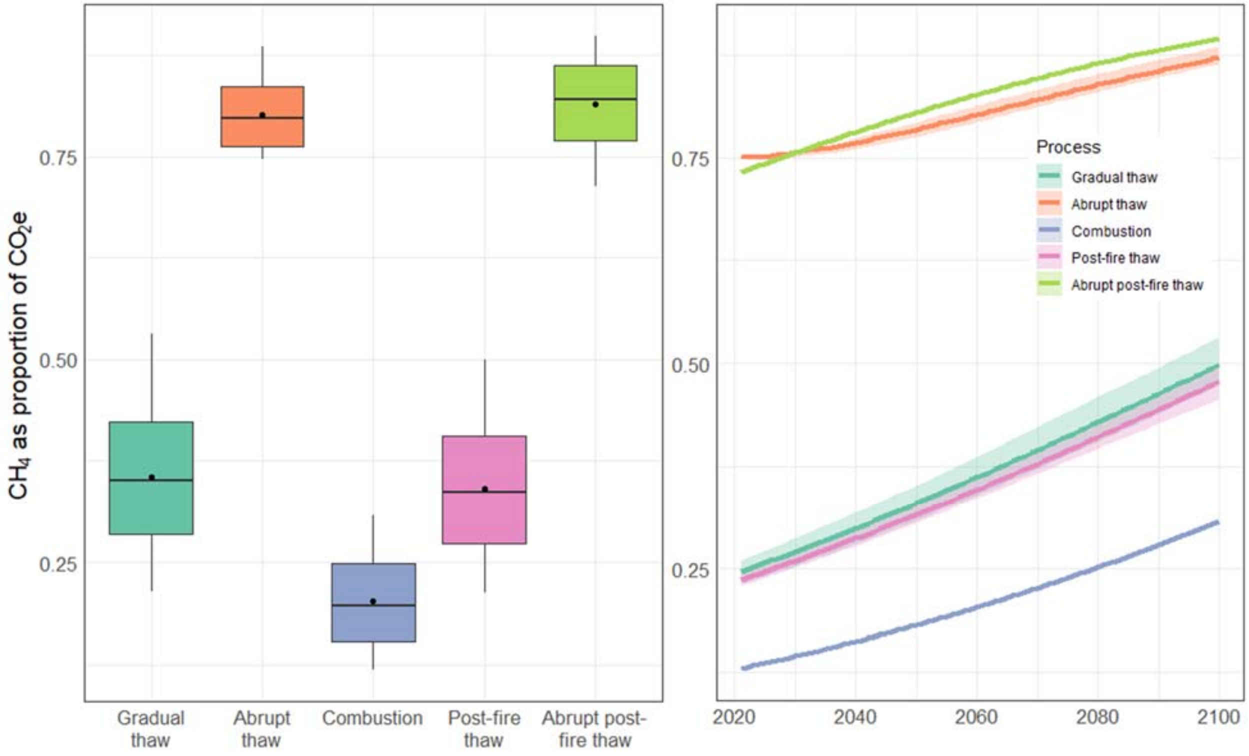

Figure 5.4: The proportion of CO_2e accounted for by CH_4, as a 2021-2100 average (left) and over time (right). Shaded areas on the right indicate the range of values across LSMs and SSP-RCP scenarios, while solid lines denote mean values. CO_2e is based on Global Warming Potential from the year of emission to 2100. Note that CH4 therefore accounts for a substantially higher proportion of CO_2e than of carbon (C) emissions, due to the higher GWP of CH_4 that is used to calculate CO_2e. Also note that, by nature, CH_4's contribution to CO_2e is higher at the end of the century due to its shorter atmospheric lifetime.

Figure S6: Annual total area affected by different stages of abrupt thaw (undisturbed area, active thaw, intermediate or stabilized thaw features, and final stage or mature thaw features), estimated using the new abrupt thaw module in OSCAR (top), and the models reported in Turetsky et al. (2020) (bottom) under SSP5-RCP8.5. Line colors indicate landscape type, following Turetsky et al. (2020).

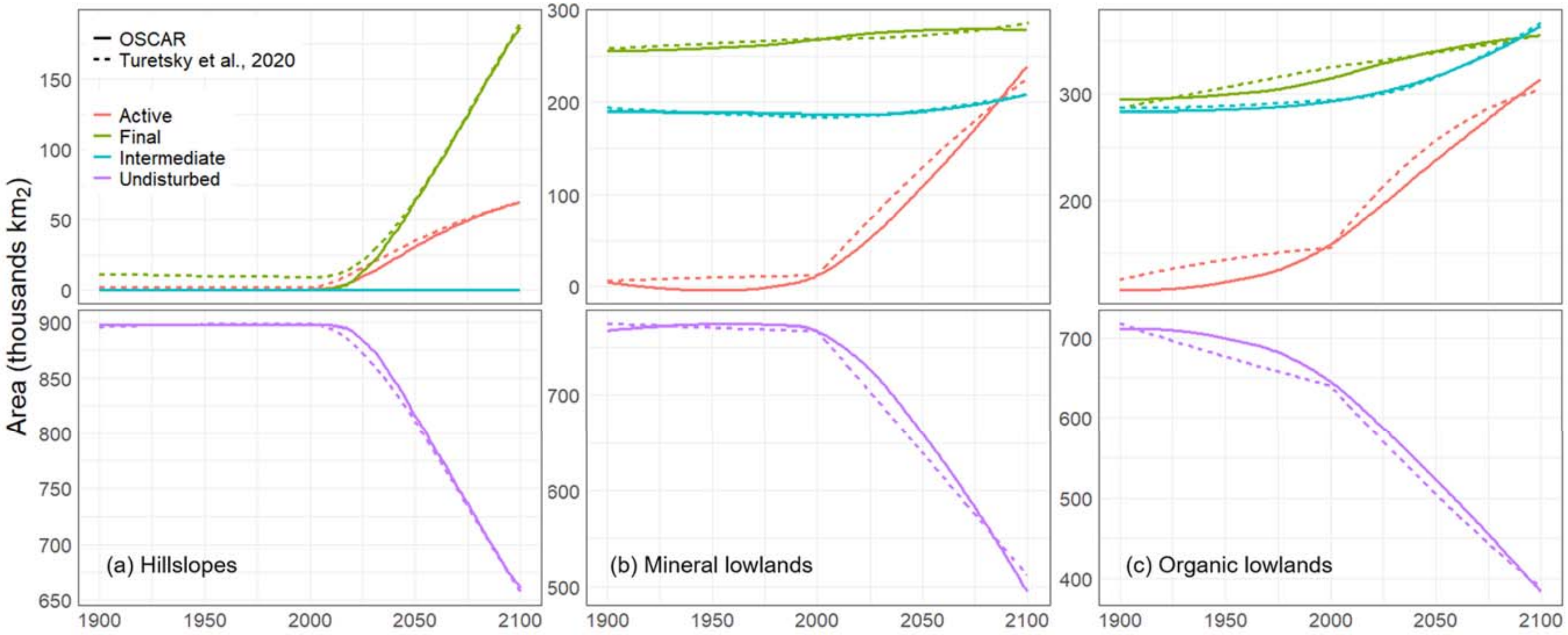

Table S1: Observational data obtained through literature searches for (a) fire impacts on active layer thickness and (b) fire impacts on ground temperature in boreal and tundra regions and used for post-fire permafrost thaw processes. Data were supplemented by unpublished datasets.

			Active Layer Thickness			**Ground temperature**			
Reference	**Biome**	**Years since fire**	Change (cm) Mean or single reported measurement	Minimum change (cm)	Maximum change (cm)	Change (°C) Mean or single reported measurement	Minimum change (°C)	Maximum change (°C)	Depth of measurement (cm)
Li et al., 2018	Boreal	1-30	92.50	20.00	300.00	1.45	-0.20	2.63	100
Nossov et al., 2013		1-4	68.00	51.00	87.00	2.20	1.50	3.00	100
Gibson et al., 2018		2-49	2.99	-0.09	8.21	4.88	1.03	7.55	40
Fisher et al., 2016		6	79.30						
Zhang et al., 2015		6	63.50						
Jiang et al., 2015		4				5.13	4.94	5.32	20
Kasischke & Johnstone 2005		1-10				9.47	6.64	11.45	20
Jafarov et al., 2013							0.00	2.20	100
Alexander et al., 2018		1	16.61	6.89	28.15	1.51	0.27	2.60	5
Burn, 1998		24				3.69			20
Williams et al., 2020		6				1.14			22
Natali et al., unpublished		11-32	17.82	2.05	41.94				
Rocha & Shaver 2011	Tundra	1-3	9.88	6.36	15.08		1.50	4.00	5
Rocha & Shaver 2011b		1				3.87	1.87	5.44	8
Rocha et al., 2012		10	6.00						
Hall et al., 1978		1	8.90						
Wein & Bliss 1973		1-2	10.25	8.00	13.00				
Liljedahl et al., 2007		1-4	16.39	5.63	26.49	1.20			100
Oechel, 1999		2-23	3.34	-0.87	9.43				
Fetcher et al., 1984		13	13.00						
Vavrek et al., 1999		24	9.00						
Patterson & Dennis 1981		2	15.00						
Barret et al., 2012		17	7.73						
Barret et al., 2012		17	4.06						
Loranty et al., 2014		41	0.00						
Jiang et al., 2015		1				2.28	1.32	3.33	20
Natali et al., unpublished		1-47	9.58	0.10	50.80				

Table S2: Data obtained through literature search used to calculate a ratio of change in ground subsidence to active layer depth, weighted by study to account for the use of multiple data points from some studies. The weighted average ratio was 0.39 (range: 0.06-2.77, standard deviation 0.59).

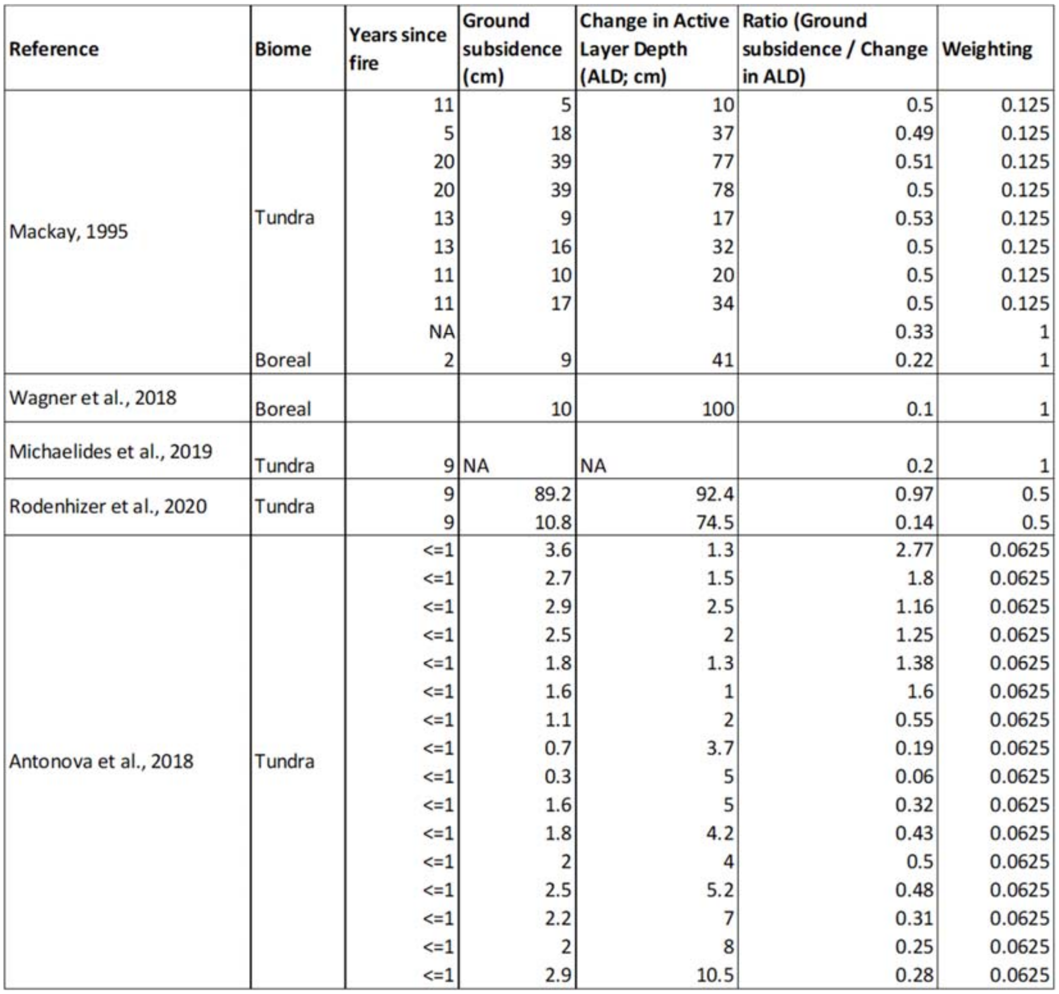

Reference	Biome	Years since fire	Ground subsidence (cm)	Change in Active Layer Depth (ALD; cm)	Ratio (Ground subsidence / Change in ALD)	Weighting
Mackay, 1995	Tundra	11	5	10	0.5	0.125
		5	18	37	0.49	0.125
		20	39	77	0.51	0.125
		20	39	78	0.5	0.125
		13	9	17	0.53	0.125
		13	16	32	0.5	0.125
		11	10	20	0.5	0.125
		11	17	34	0.5	0.125
		NA			0.33	1
	Boreal	2	9	41	0.22	1
Wagner et al., 2018	Boreal		10	100	0.1	1
Michaelides et al., 2019	Tundra	9	NA	NA	0.2	1
Rodenhizer et al., 2020	Tundra	9	89.2	92.4	0.97	0.5
		9	10.8	74.5	0.14	0.5
Antonova et al., 2018	Tundra	<=1	3.6	1.3	2.77	0.0625
		<=1	2.7	1.5	1.8	0.0625
		<=1	2.9	2.5	1.16	0.0625
		<=1	2.5	2	1.25	0.0625
		<=1	1.8	1.3	1.38	0.0625
		<=1	1.6	1	1.6	0.0625
		<=1	1.1	2	0.55	0.0625
		<=1	0.7	3.7	0.19	0.0625
		<=1	0.3	5	0.06	0.0625
		<=1	1.6	5	0.32	0.0625
		<=1	1.8	4.2	0.43	0.0625
		<=1	2	4	0.5	0.0625
		<=1	2.5	5.2	0.48	0.0625
		<=1	2.2	7	0.31	0.0625
		<=1	2	8	0.25	0.0625
		<=1	2.9	10.5	0.28	0.0625

Table S3: Emissions [add caption]

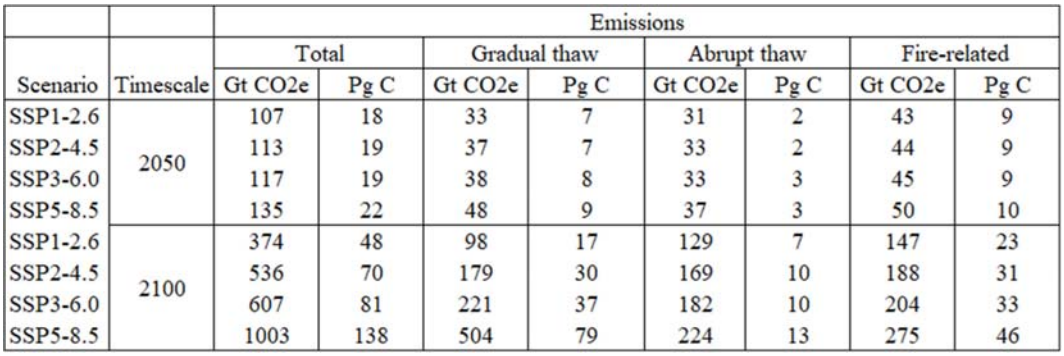

		Emissions							
		Total		Gradual thaw		Abrupt thaw		Fire-related	
Scenario	Timescale	Gt CO2e	Pg C	Gt CO2e	Pg C	Gt CO2e	Pg C	Gt CO2e	Pg C
SSP1-2.6	2050	107	18	33	7	31	2	43	9
SSP2-4.5		113	19	37	7	33	2	44	9
SSP3-6.0		117	19	38	8	33	3	45	9
SSP5-8.5		135	22	48	9	37	3	50	10
SSP1-2.6	2100	374	48	98	17	129	7	147	23
SSP2-4.5		536	70	179	30	169	10	188	31
SSP3-6.0		607	81	221	37	182	10	204	33
SSP5-8.5		1003	138	504	79	224	13	275	46

Table S4: Detailed carbon budget estimates in Gt CO_2e. An asterisk (*) means no budget could be estimated for this combination of temperature goal and future climate scenario. Permafrost and wildfire representation indicates which permafrost thaw and wildfire processes are ‘switched on’; A = gradual thaw only; B = gradual and abrupt thaw; C = gradual and abrupt thaw, and below-ground combustion; D = all processes.

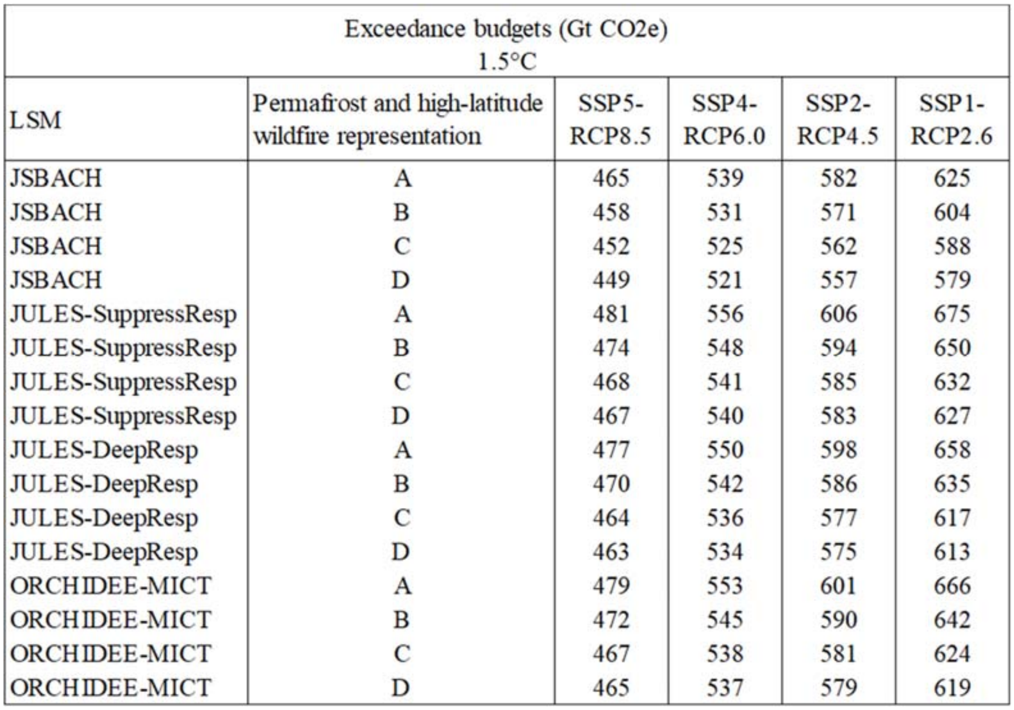

Exceedance budgets (Gt CO2e) 1.5°C					
LSM	Permafrost and high-latitude wildfire representation	SSP5-RCP8.5	SSP4-RCP6.0	SSP2-RCP4.5	SSP1-RCP2.6
JSBACH	A	465	539	582	625
JSBACH	B	458	531	571	604
JSBACH	C	452	525	562	588
JSBACH	D	449	521	557	579
JULES-SuppressResp	A	481	556	606	675
JULES-SuppressResp	B	474	548	594	650
JULES-SuppressResp	C	468	541	585	632
JULES-SuppressResp	D	467	540	583	627
JULES-DeepResp	A	477	550	598	658
JULES-DeepResp	B	470	542	586	635
JULES-DeepResp	C	464	536	577	617
JULES-DeepResp	D	463	534	575	613
ORCHIDEE-MICT	A	479	553	601	666
ORCHIDEE-MICT	B	472	545	590	642
ORCHIDEE-MICT	C	467	538	581	624
ORCHIDEE-MICT	D	465	537	579	619

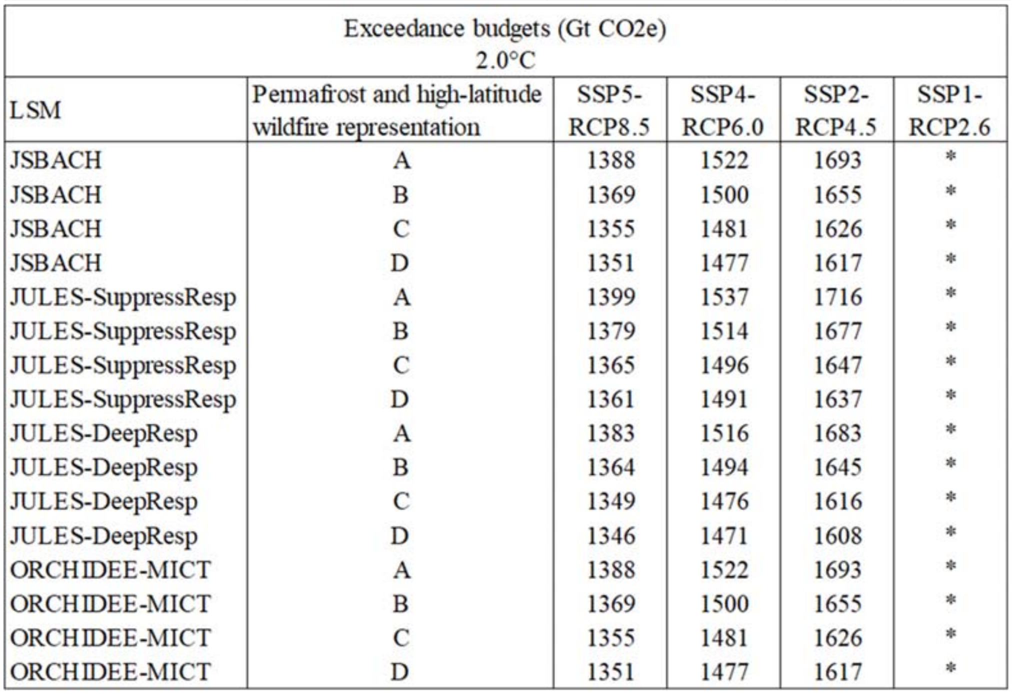

Exceedance budgets (Gt CO2e) 2.0°C					
LSM	Permafrost and high-latitude wildfire representation	SSP5-RCP8.5	SSP4-RCP6.0	SSP2-RCP4.5	SSP1-RCP2.6
JSBACH	A	1388	1522	1693	*
JSBACH	B	1369	1500	1655	*
JSBACH	C	1355	1481	1626	*
JSBACH	D	1351	1477	1617	*
JULES-SuppressResp	A	1399	1537	1716	*
JULES-SuppressResp	B	1379	1514	1677	*
JULES-SuppressResp	C	1365	1496	1647	*
JULES-SuppressResp	D	1361	1491	1637	*
JULES-DeepResp	A	1383	1516	1683	*
JULES-DeepResp	B	1364	1494	1645	*
JULES-DeepResp	C	1349	1476	1616	*
JULES-DeepResp	D	1346	1471	1608	*
ORCHIDEE-MICT	A	1388	1522	1693	*
ORCHIDEE-MICT	B	1369	1500	1655	*
ORCHIDEE-MICT	C	1355	1481	1626	*
ORCHIDEE-MICT	D	1351	1477	1617	*

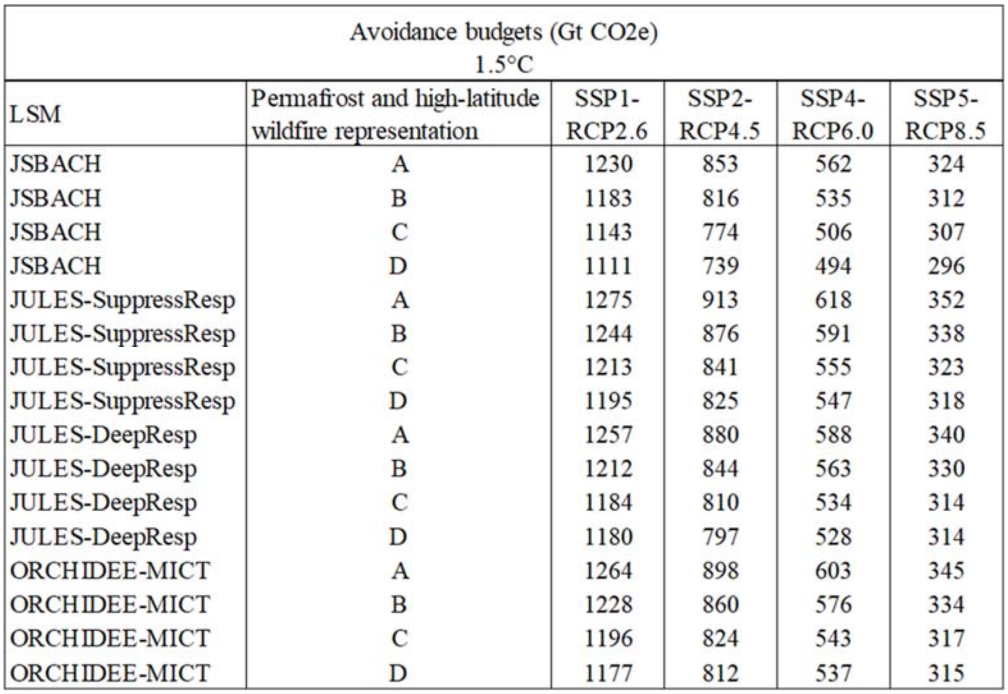
Avoidance budgets (Gt CO2e)
1.5°C

LSM	Permafrost and high-latitude wildfire representation	SSP1-RCP2.6	SSP2-RCP4.5	SSP4-RCP6.0	SSP5-RCP8.5
JSBACH	A	1230	853	562	324
JSBACH	B	1183	816	535	312
JSBACH	C	1143	774	506	307
JSBACH	D	1111	739	494	296
JULES-SuppressResp	A	1275	913	618	352
JULES-SuppressResp	B	1244	876	591	338
JULES-SuppressResp	C	1213	841	555	323
JULES-SuppressResp	D	1195	825	547	318
JULES-DeepResp	A	1257	880	588	340
JULES-DeepResp	B	1212	844	563	330
JULES-DeepResp	C	1184	810	534	314
JULES-DeepResp	D	1180	797	528	314
ORCHIDEE-MICT	A	1264	898	603	345
ORCHIDEE-MICT	B	1228	860	576	334
ORCHIDEE-MICT	C	1196	824	543	317
ORCHIDEE-MICT	D	1177	812	537	315

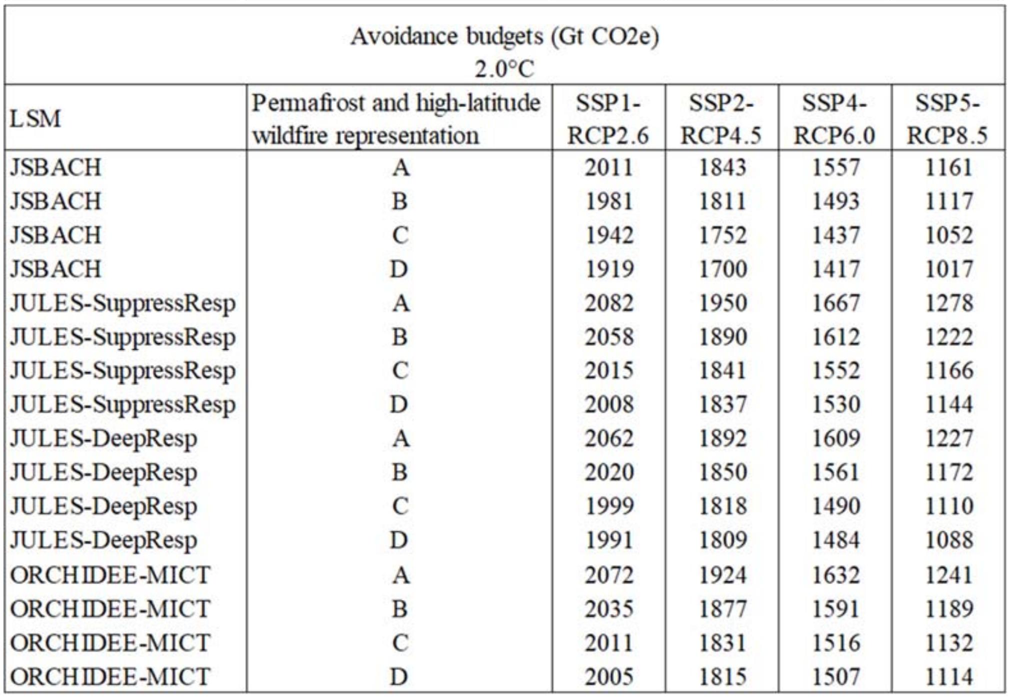
Avoidance budgets (Gt CO2e)
2.0°C

LSM	Permafrost and high-latitude wildfire representation	SSP1-RCP2.6	SSP2-RCP4.5	SSP4-RCP6.0	SSP5-RCP8.5
JSBACH	A	2011	1843	1557	1161
JSBACH	B	1981	1811	1493	1117
JSBACH	C	1942	1752	1437	1052
JSBACH	D	1919	1700	1417	1017
JULES-SuppressResp	A	2082	1950	1667	1278
JULES-SuppressResp	B	2058	1890	1612	1222
JULES-SuppressResp	C	2015	1841	1552	1166
JULES-SuppressResp	D	2008	1837	1530	1144
JULES-DeepResp	A	2062	1892	1609	1227
JULES-DeepResp	B	2020	1850	1561	1172
JULES-DeepResp	C	1999	1818	1490	1110
JULES-DeepResp	D	1991	1809	1484	1088
ORCHIDEE-MICT	A	2072	1924	1632	1241
ORCHIDEE-MICT	B	2035	1877	1591	1189
ORCHIDEE-MICT	C	2011	1831	1516	1132
ORCHIDEE-MICT	D	2005	1815	1507	1114